Indian Journal of Pure & Applied Physics
Vol. 43, January 2005, pp. 44-50

Mössbauer, X-ray and magnetization studies of $Ni_{0.5}Zn_{0.5}Al_xFe_{2-x}O_4$ system

Suman*, Roshan Lal*, N D Sharma*, S P Taneja** & Ajay Gupta***
*Department of Physics, Kurukshetra University, Kurukshetra 136 119
**Department of Physics, Maharshi Dayanand University, Rohtak 124 001
***Inter University Consortium for DAE Facilities, Khandwa Road, Indore 452 017

Received 9 August 2004; revised 27 October 2004; accepted 29 October 2004

The structural and magnetic properties of the mixed spinel system $Ni_{0.5}Zn_{0.5}Al_xFe_{2-x}O_4$ (x=0.0,0.2,0.4,0.6,0.8 and 1.0) have been investigated by X-ray diffraction, magnetization and Mössbauer measurements. The variation of Mössbauer parameters, lattice parameters and crystalline size of the products formed with variation in the composition of Fe and Al ratio has been studied. The studies confirm the formation of nano-size ferrite particles. It is observed that lattice parameters decrease, with increasing aluminium concentration. A ferromagnetic relaxation occurs when x is increased to 0.6, which is followed by weak paramagnetic transition. With further increase of x to 1.0 the system again shows weak ferromagnetism. The decrease in magnetic hyperfine field with increase in Al concentration has been explained on the basis of super transferred hyperfine field. The variation of the saturation magnetic moment per formula unit measured at 300 K decreases with Al concentration x, suggesting the decrease in ferromagnetic behaviour. These observations indicate the existence of a non-collinear structure in a nano-particles ferrite system. The non-collinear structure in this system is also verified by Neel's two sub-lattice model.

[**Keywords:** Mössbauer study, X-ray diffraction, Mixed spinel system, $Ni_{0.5}Zn_{0.5}Al_xFe_{2-x}O_4$]
IPC Code: G01N 23/00, 24/00

1 Introduction

Ferrites are widely used in microwave and electrical industries. These are technologically important materials because of their interesting physical and chemical properties, which arise due to their ability to distribute the cations among the available octahedral B and tetrahedral A-sites. The magnetic as well as the electrical properties of the spinel ferrites are governed by the type of the magnetic ion residing on the A and B-sites and the relative strength of magnetic interactions. When A-B inter-sub-lattice interactions are much stronger than the A-A and B-B intra-sublattice interactions the spins have a collinear structure in which the moments on the A-sites are antiparallel to the moments on the B-sites. Some work has been reported earlier on magnetic properties of aluminium substituted ferrites like $CoFe_2O_4$ (Ref.1), $MgFe_2O_4$ (Ref.2) and $NiFe_2O_4$ (Ref.3) prepared by ceramic process, whose applications are limited as their particle size remains uncontrolled in such techniques. Recently, more attention has been focused on the preparation and characterization of Mn substituted Ni-Zn ferrites[4]. In the present paper, the effect of Al^{3+} substitution on the magnetic properties of $Ni_{0.5}Zn_{0.5}Al_xFe_{2-x}O_4$ spinel system using X-ray, magnetization and Mössbauer measurements has been studied. The mean size of the nano-particles can be monitored through controlling the concentration of the reagents, therefore, such ferrites in nano-particle range offer excellent opportunities to many recent technologies[5].

*E-mail- physik@granth.kuk.ernet.in

2 Experimental Details

2.1 Sample preperation

Six samples of Al^{3+} substituted $Ni_{0.5}Zn_{0.5}Al_xFe_{2-x}O_4$ spinel ferrite system were synthesized by citrate precursor method. The starting materials were AR grade nickel nitrate (99%), zinc nitrate (99%), aluminium nitrate (99%), iron(III) citrate(99%) and citric acid (99%) supplied by s d fine India. The chemicals were weighed in stoichiometric proportion. Iron(III) citrate solution was prepared in distilled water by heating at 40°C with constant stirring. Citric acid, with a few drops of water, was added separately to nickel nitrate, zinc nitrate and aluminium nitrate. The solutions were heated at 40°C for about 15 min and then added to the iron citrate solution under continuous stirring. The mixture was evaporated to dryness to obtain a transparent brown colour glossy material, containing the constituent metal ions homogeneously mixed at the atomic level. The obtained powders were calcined at 500C for 1 hr.

2.2 X-ray measurements

The X-ray diffraction patterns were recorded using Cu-K_α radiation (angle range 20° to 80°) on a Philips X-ray diffractometer. The diffraction patterns show the sharp lines corresponding to a single-phase spinel for all the samples.

2.3 Magnetization measurements

The magenetization measurements of all samples were carried out at room temperature using vibrating sample magnetometer (VSM).

2.4 Mössbauer measurements

Samples were crushed to obtain fine powder and sieved through a 200 μm gauge. The Mössbauer absorber was prepared by pressing the powder in an aluminium holder of diameter 10 mm so that areal density was 50mg/cm^2 with uniform spread and fixing the open ends with cellophane tapes. The absorption spectra were recorded in transmission geometry at room temperature with a constant acceleration Mössbauer drive and a 256-multi-channel analyzer, using Austin Science Inc, USA Mössbauer Spectrometer. A single line ^{57}Fe(Rh) source with initial activity of 10 mCi was used. In general several runs were taken to check the reproducibility of the spectra. Total counts collected per channel were close to 10^6 or more. The Mössbauer spectrometer was calibrated using a 0.001 inch enriched α-Fe foil. The outermost lines were separated through 10.68mm/s. This is in excellent agreement with an ideal absorption spectrum and calibration was done accordingly. One channel corresponds to a velocity of 0.0628mm/s. The experimental data were computer fitted using a least squares fitting program assuming Lorentzian lineshape with χ^2 minimization technique. The solid line through the data points is the result of the computer fit of the data.

3 Results and Discussion

Six samples of the mixed spinel system $Ni_{0.5}Zn_{0.5}Al_xFe_{2-x}O_4$; x=0.0, 0.2, 0.4, 0.6, 0.8 and 1.0 were studied. In each sample two of the constituents i.e. Ni and Zn were fixed while Fe was replaced by aluminium.

3.1 X-ray measurements

In Fig. 1, the recorded X-ray diffraction patterns for all compositions of $Ni_{0.5}Zn_{0.5}Al_xFe_{2-x}O_4$ show all those lines, which belong to the cubic spinel structure. The reflection from the planes (220), (311), 222), (400), (422), (333), (533) and (622) appears for all the samples. The appearance of these planes proved that the samples are spinel ferrites and have only a single cubic phase[6]. The interplanr distance d (Å) was calculated using Bragg's law and the values of lattice constant a (Å) were determined with an accuracy of ± 0.002 Å using the following relation:

$$a = d_{hkl}\sqrt{(h^2 + k^2 + l^2)}$$

and are shown in Table 1. The lattice constant a (Å) decreases linearly with increasing Al content x as shown in Fig. 2. Thus obeying the Vegard's law[7], which may be attributed to the replacement of larger

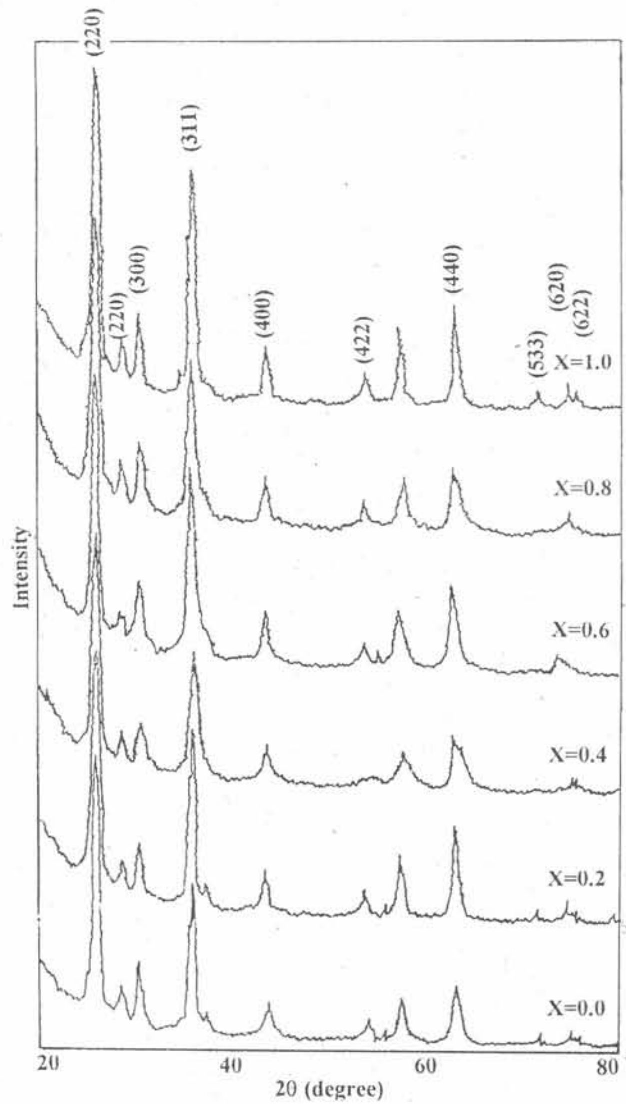

Fig. 1—XRD pattern of $Ni_{0.5}Zn_{0.5}Al_xFe_{2-x}O_4$ system at room temperature

Table 1—Lattice constant, X-ray density, particle size, saturation magnetization, corecivity, retentivity, magnetone number for $Ni_{0.5}Zn_{0.5}Al_xFe_{2-x}O_4$ system

Content x	Lattice constant a (Å)	X-Ray density (d_x)	Particles size (nm)	Ms (emu/mol) 300 K	n_B (μ_B) 300 K	Coercivity H_C	Retentivity M_r	n_B^N(μ_B)
0.0	8.3485	5.43	11.39	3684.70	2.14	69.09	1007.44	5.3
0.2	8.3433	5.31	11.39	2753.83	1.59	21.54	253.97	4.97
0.4	8.3264	5.20	11.39	2368.69	1.36	7.36	59.77	4.7
0.6	8.3201	5.08	10.36	993.93	0.57	2.71	21.52	4.2
0.8	8.3054	4.98	10.38	1313.35	0.75	4.80	30.45	4.01
1 .0	8.295	4.86	11.47	1396.52	0.79	7.65	46.32	3.73

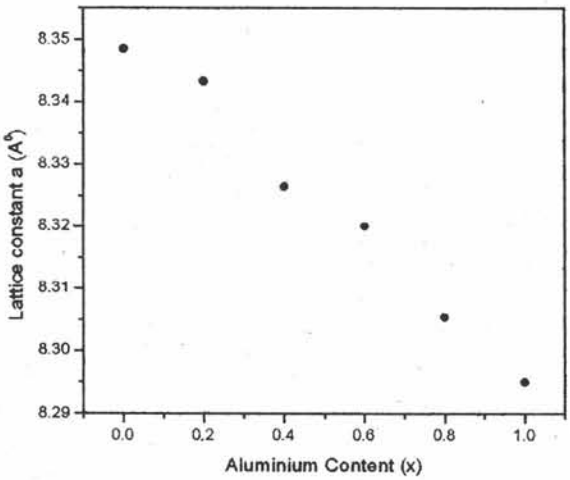

Fig. 2—Variation of lattice constant a (Å) with aluminium content (x)

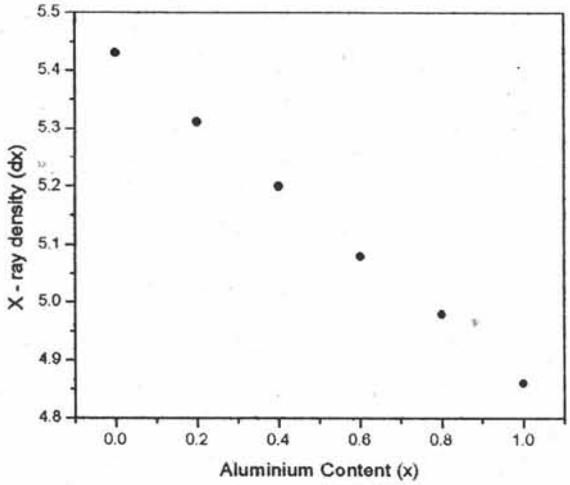

Fig. 3—Variation of X-ray density with aluminium content (x)

Fe^{3+} ions (0.64Å) by smaller Al^{3+}ions (0.51Å) in the $Ni_{0.5}Zn_{0.5}Al_xFe_{2-x}O_4$ system. The X-ray density (d_X) for each sample was calculated by using the relation:

$$d_X = Z\,M/N\,V$$

where Z is the number of molecules per unit cell (Z= 8), M molecular weight, V unit cell volume and N is Avogadro number.

The compositional dependence of X-ray density (d_X) is shown in Fig. 3. The X-ray density (d_X) decreases with increasing aluminium concentration (x). This is because the decrease in mass overtakes the decrease in volume of the unit cell. The broad XRD lines indicate that the ferrite particles are of nanosize[8]. The average particle size of each sample was determined from the line broadening of the (311) peaks using Scherrer equation[9] :

$$d = 0.9\,\lambda\,/\,B\,(\cos\theta)$$

where B is line width , λ the wavelength and θ is the angle of reflection.

It was observed that the average particle size of each sample lies in nano-particle range and it abruptly changes with increasing Al concentration as shown in Table 1.

3.2 Magnetization measurements

The magneton number (nB) was calculated from the hysteresis data (M-H curve) obtained at 300K by the following relation[10]:

n_B = molecular weight × saturation magnetization / 5585

μ_B = saturation magnetization × molecular weight / 5585 ds

The variation of n_B (the saturation magnetization per formula unit in Bohr magneton μ_B) was obtained from hysteresis loop technique as a function of Al concentration and is shown in Table 1. From the field dependence of magnetization and the observed magnetic moments at room temperature, it is evident that n_B decreases with increase of aluminium concentration. From B-H loop the remanence induction (retentivity M_r) and the coercivity (H_C) were determined. It is observed that the values of retentivity M_r and coercivity (H_C) decrease with increasing aluminium concentration i.e. when x approaches 0.4, these values indicate the ferromagnetic behaviour of the samples. On increasing x to 0.6, the values of retentivity M_r and coercivity (H_C) become smaller and the hysteresis loop perfectly passes through the center as shown in Fig. 4, which clearly support the paramagnetic nature of the sample. When the value of x is increased from 0.8 and 1.0 the values of retentivity (M_r) and coercivity (H_C) slightly increase which suggest that the paramagnetic character again changes to ferromagnetic. The decrease of saturation magnetization with increase of aluminium concentration also shows a similar trend and the similar variation is also observed in the particle size. From the above results, it is concluded that in ferrites having nano-particles, the reduction of magnetization depends upon the particle size[8].

According to Neel's two sublattice model[11], the magnetic moment per formula unit, η_B^N, with the known cation distribution at A and B sites is given by following equation:

$$\eta_B^N = M_B(x) - M_A(x) \quad \ldots (1)$$

where η_B^N is the Neel magnetic moment per formula unit in μ_B, M_B and M_A are respectively the B and A sub-lattice magnetic moment in μ_B. $\eta_B{}^N{}_{(x)}$ is the calculated value of magnetic moment using Neel's model and x is dopant concentration.

The values of $\eta_B{}^N{}_{(x)}$ obtained at room temperature cannot be compared with $\eta_{B(x)}{}^N$ values calculated according to Neel's model at 0 K. However, the ratio of magnetic moments i.e. $\eta_{B(x)}/\eta_{B(0)}$ can be compared with $\eta_{B(x)}{}^N/\eta_{B(0)}{}^N$ and a disagreement is observed between them. This indicates that significant canting exists on B sites leading to a non-collinear type of magnetic structure[12].

Information on the cation distribution can be derived from the magnetization, X-ray diffraction and area ratio of the A and B-sites observed from the Mössbauer absorption spectra[13], this has been found as follows:

For $x = 0.0$
$(Zn_{0.40}Fe_{0.55}Ni_{0.05})^A[Zn_{0.1}Ni_{0.45}Fe_{1.54}]^BO_4^{-2}$
For $x=0.2$
$(Zn_{0.425}Fe_{0.475}Ni_{0.07}Al_{0.03})^A[Zn_{0.075}Ni_{0.43}Fe_{1.325}Al_{0.17}]^BO_4^{-2}$
For $x=0.4$
$(Zn_{0.445}Fe_{0.4}Ni_{0.075}Al_{0.08})^A[Zn_{0.055}Ni_{0.425}Fe_{1.2}Al_{0.32}]^BO_4^{-2}$
For $x=0.6$
$(Zn_{0.465}Fe_{0.35}Ni_{0.075}Al_{0.11})^A[Zn_{0.037}Ni_{0.425}Fe_{1.05}Al_{0.49}]^BO_4^{-2}$
For $x = 0.8$
$(Zn_{0.485}Fe_{0.255}Ni_{0.11}Al_{0.15})^A[Zn_{0.015}Ni_{0.39}Fe_{0.945}Al_{0.65}]^BO_4^{-2}$
For $x = 1.0$
$(Zn_{0.495}Fe_{0.175}Ni_{0.13}Al_{0.20})^A[Zn_{0.005}Ni_{0.37}Fe_{0.825}Al_{0.80}]^BO_4^{-2}$ ... (2)

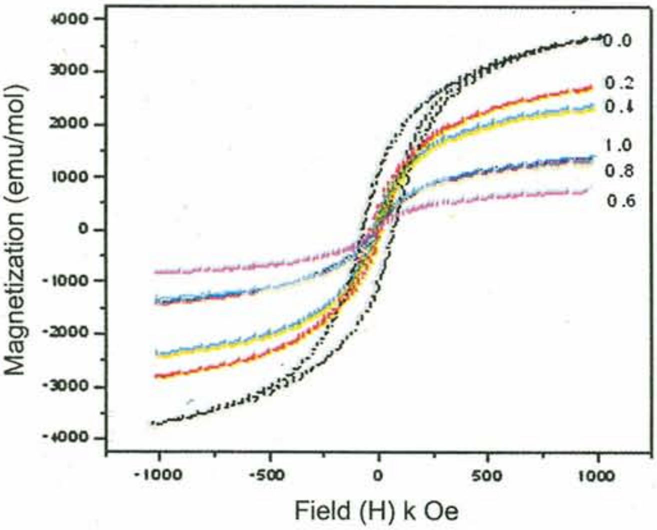

Fig. 4—Field dependence of magnetization curve (M-H) at 300 K for $Ni_{0.5}Zn_{0.5}Al_xFe_{2-x}O_4$

The possible values of magnetic moment per formula unit ($\eta_B{}^N{}_{(x)}$) calculated from Neel's model on the basis of cation distribution as taken from the literature[3,21] for x=0.0 to 1.0 using Eqs 1 and 2 are shown in Table 1. The calculated ($\eta_B{}^N{}_{(x)}$) values for x=0 to 1.0 disagree with the experimentally found n_B values (Table 1) which confirms a non-collinear[2,14-15] magnetic structure due to significant canting that exists on B-site.

In addition to the deviation from normal cation distribution, many other factors reported in the literature may contribute to the reduction of M_s in nano-particles. One can attribute the smaller values of M_s in nano-particles to the existence of random canting of particle surface spins caused by competing anti-ferromagnetic exchange interactions due to asymmetry in the environment of these spins[16]. The lower magnetization values are due to non-saturation effects because of random distribution of the small particles with enhanced values of magneto-crystalline anisotropy. In addition to these effects, disorder cation distribution[17-18] formation of a dead layer on the surface[19] can also explain the reduced M_s in nano-particles.

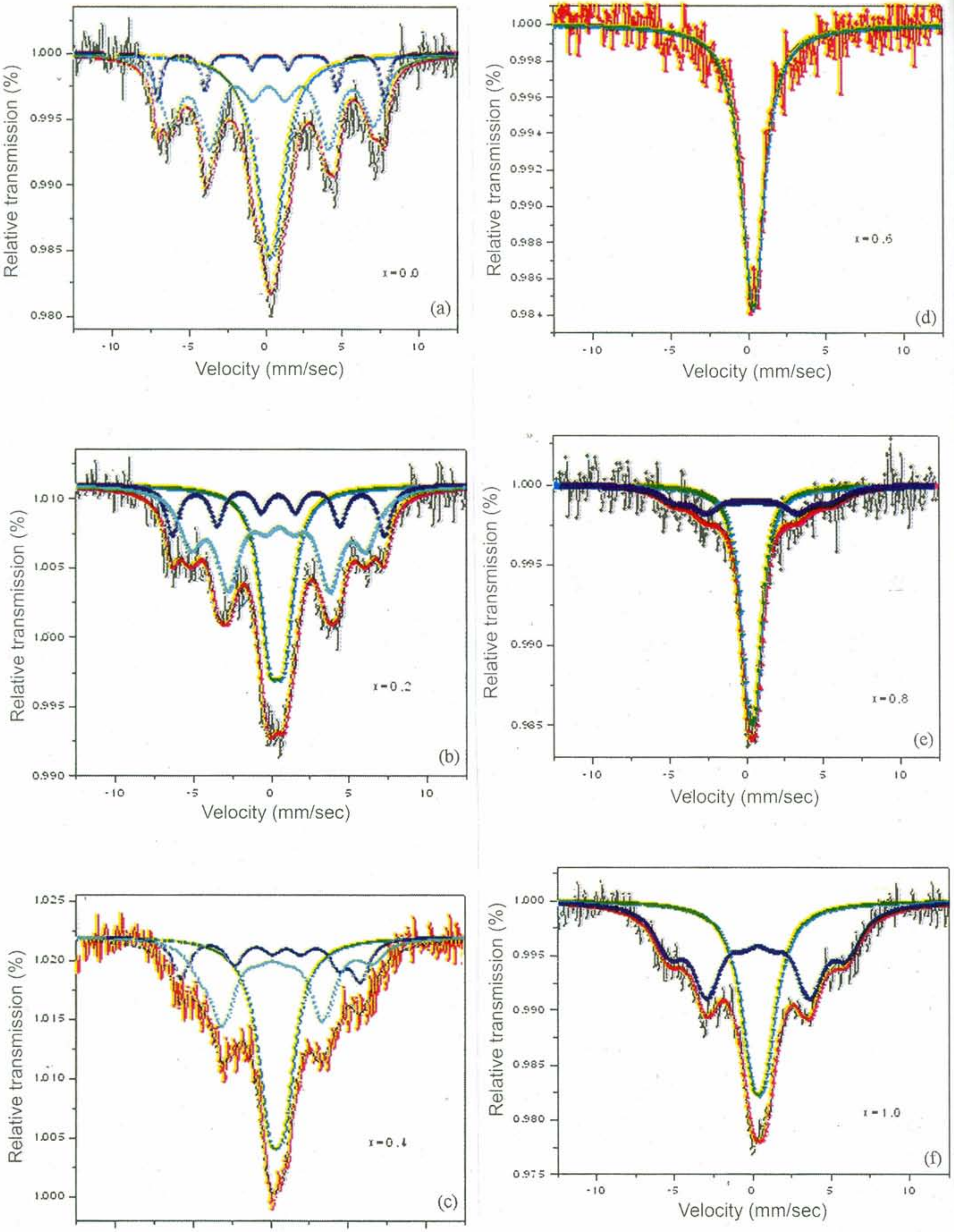

Fig. 5—Mössbauer absorption spectrum recorded at 300 K for x = 0.0, 0.2, 0.4, 0.6, 0.8 and 1.0 samples

3.3 Mössbauer measurements

Mössbauer absorption spectra for all the samples i.e. x=0.0, 0.2, 0.4, 0.6, 0.8 and 1.0 were recorded at room temperature as shown in Fig. 5. The spectra were computer fitted and the hyperfine parameters e.g. isomer shift δ, quadrupole splitting Δ, line width Γ and hyperfine field H_{int} were computed using normal procedure and are listed in Table 2. The Mössbauer spectra (Fig. 5) exhibit two magnetic hyperfine split sextets besides a broad doublet. One sextet due to the Fe^{3+} ion at the tetrahedral (A) sites and the outer sextet is due to the Fe^{3+} ions at the octahedral sites, which indicate ferromagnetic behaviour of the samples in agreement with the magnetization results (Table 1) for $x \leq 0.4$. The central doublet in all the samples arises due to the presence of non-magnetic zinc ion[12,20,28]. It is known[20] that Zn and Ni ions occupy A and B-sites respectively. Although iron and aluminium ions co-exist at both A and B-sites, however, they prefer the B-sites. On addition of Al^{3+} (non-magnetic ion) which enters the octahedral site, and slightly broadens the line width and reduces the intensity of the central doublet. The quadrupole splitting values for $x \leq 0.4$ are found to be zero (Table 2) due to the co-existence of chemical disorder and an overall cubic symmetry in the spinel system. When the concentration of Al^{3+} ions, (x is further increased to 0.6) increases the spectrum collapses to a doublet and a weak hyperfine field exists at lattice sites, which cannot be computer fitted as shown in Fig. 5.

As the Al^{3+} concentration increases further, the intensity of distributed magnetic hyperfine field increases, which suggests that the paramagnetic character changes to ferromagnetic character. It has been observed that the internal magnetic field decreases at A as well as at B-site with the increase in Al concentration. Such a variation can be qualitatively explained on the basis of supertransfered hyperfine field[21]. As Al^{3+} ions have got a strong tendency to occupy B-site[22], it reduces AB interaction with increase in Al concentration. As the Al concentration

Table 2—Hyperfine interaction parameters computed from the Mössbauer absorption spectra recorded at room temperature, isomer shift is given relative to α–Fe.

Composition (x)	Site	I S (δ ± 0.01) mm/sec	Q S (Δ± 0.01) mm/sec	Area ± 0.2 mm/sec	H_{int} ± 2.0 k Oe
	—	0.29	0.85	25.8	—
0.0	A	0.28	0.0	34.8	38.88
	B	0.32	0.1	39.4	43.91
	—	0.29	0.94	34.24	—
0.2	A	0.30	0.00	28.87	34.92
	B	0.33	0.01	36.89	41.34
	–	0.30	0.95	53.49	—
0.4	A	0.29	0.0	23.19	27.88
	B	0.32	0.0	34.32	36.81
0.6	—	0.28	0.81	100	—
0.8	—	0.29	0.89	64.15	—
	B	0.30	0.0	35.85	30.06
1.0	—	0.29	0.94	69.59	—
	B	0.31	0.0	30.41	42.77

is increased, the BB supertransfered hyperfine interactions become comparable in strength because of canting of spins (non-collinear). These BB supertransfered hyperfine interactions are strongly dependent on the spins and therefore reduce the net hyperfine field[23]. It has also been observed from Mössbauer results that the area under B and A site decreases with increase of Al concentration due to which ferromagnetic character decreases to weak paramagnetic. On further increase of Al, it again changes to weak ferromagnetic, this is due to the existence of canting among spins of B-site ions, which was responsible for variation of saturation magnetization without any evidence of presence of the iron clusters. In spinel ferrites, the magnetic Fe^{3+} ion concentration on A-site remains lower compared to that on B sites. These ions are distributed over A and B- sites and experience different hyperfine fields. This causes the decrease in hyperfine field of tetrahedral and octahedral sites almost at equal rates with increasing Al concentration. The relaxation effects[23-24]in Mössbauer spectra arise due to domain-wall displacement.

In our present investigation, the possible interactions at the B–site are as follows: (1) Fe^{3+}-Fe^{3+}, (2) Fe^{3+}-Ni^{2+}, (3) Fe^{3+}-Al^{3+}, (4) Al^{3+}-Al^{3+}, (5) Ni^{2+}-Ni^{2+}, (6) Ni^{2+}-Al^{3+}. Out of these Fe^{3+}-Fe^{3+} and Fe^{3+}-Ni^{2+} interactions are very weak[27-28,] while Fe^{3+}-Al^{3+}, Al^{3+}-Al^{3+}, Ni^{2+}-Ni^{2+} and Ni^{2+}-Al^{3+} interactions are very strong and anti-ferromagnetic[25-27]. As the Al ion replaces the iron ion at B-site, it reduces the Fe^{3+} concentration at the B-site. Thus, metal-metal interactions at B-site are reduced which cause depletion in area ratio of B and A-sites observed from the Mössbauer spectra. This indicates non-collinear structure. It is also evident from the Mössbauer spectra that there is systematic decrease in the internal hyperfine field H_{in} values with the increasing aluminium substitution. This happens because the replacements of larger Fe^{3+} ions (0.64) by smaller Al^{3+} ions (0.51) influence the internal hyperfine fields at the nearest Fe^{3+} sites through transferred hyperfine fields.

3 Conclusion

The system $Ni_{0.5}Zn_{0.5}Al_xFe_{2-x}O_4$ shows ferromagnetic to weak paramagnetic behaviour when x approaches to 0.6. When x further increases to 1.0 the system again shows a weak ferromagnetic behaviour. The values of magnetic moment per formula unit obtained from B-H curve at room temperature are different and thus confirm non-collinear structure. This is in agreement with Mössbauer observations. It is thus concluded that a non-collinear magnetic structure exists in ferrites of nano-particles.

Acknowledgement

The authors wish to thank Dr H K Sharma, Department of Chemistry, Kurukshetra University, Kurukshetra, for his help in preparing the ferrite samples. The authors are also grateful to Dr Alok Banerji, Scientist, IUC, DAE Facilities, Indore, for his cooperation in carrying out the magnetization work.

References

1 Mostafa F M & Suwalski J, *Indain J of Pure & Appl Phys*, 24 (1986) 411.
2 Modi Kunal B, Jani N N & Joshi H H, *Indain J of Pure & Appl Phys*, 33 (1995) 758.
3 Mundada O G, Modi Kunal B, Jadhav K M & Bichile G K, *Indain J of Pure & Appl Phys*, 35 (1997) 554.
4 Singh Amarendra K, Goel T C, Mendiratta R G, Thakur O P and Chander Parkash, *J Appl Phys*, 92 7 (2002) 3872.
5 Liu Chao, Rondinone Adam J & Zhang John Z, *Pure Appl Chem*, 72 1-2 (2000) 37.
6 Amer M A, *Phys stat sol (a)*, 181 (2000) 539.
7 Whinfrey C G, Eckort D W & Tauber A, *J Am Chem Soc*, 82 (1960) 2695.
8 Suresh K & Patil K C, *J Mater Sc Lett*, 13 (1994) 1712.
9 Cullity B D, *Elements of X-ray Diffraction*, Addison-Wesley Publishing Company, Inc. USA (1956).
10 Smit, *Magnetic properties of Materials*, (McGraw Hill Book Co) (1971) 89.
11 Neel L,*C R Acad Sci*, 230 (1950) 375.
12 Rao A D P, Raju S B, Vadera S R & Sharma D R, *Bull Mater Sci*, 26 5 (2003) 505.
13 Mahmoud M H, Hamdeh H H , Ho J C, O'Shea M J & Walker J C, *J Mag & Mag Mater*, 220 (2000) 139.
14 Jani N N, Trivedi B S, Joshi H H, Bichile G K & Kulkarni R G, *Bull Mater Sci*, 21 3 (1998) 233.
15 Shukla S J, Jadhav K M & Bichile G K, *Indain J of Pure & Appl Phys*, 39 (2001) 226.
16 Pankhurst Q A & Polland R G, *Phys Rev Lett*, 67 (1991) 248.
17 Vollath D, Szabu D V, Taylor R D & Wills J U, *J Mag Mag Mater*, 12 (1997) 2175.
18 Morrish A H, Li Z W & Zhou Z X, *J Phys (Paris)* C1, (1997) 513.
19 Chen J P Sorensen C M, Klabunde K J, & Hadjipanayis G C, *Phys Rev B*, 54 (1996) 9288.
20 Yang De Ping, Lavoie Lindsey K, Zhang Yide, Zhang Zonglao & Ge Shinhui, *J Appl Phys*, 93,10(2003).
21 Woude F Vander & Sawatzky G A, *Phys Rev B* (USA), 4 (1971) 3159.
22 Romeijn F C, *Philips Res Ref (Netharlands)*, 8 (1953) 304.
23 Srivastava C M, Shringi S N & Srivastava R G, *Phys Rev B*, 14 (1976) 2041.
24 Srivastava C M, Shringi S N & Srivastava R G & Nandikar N G, *Phys Rev B*, 14 (1976) 2032.
25 Blasse G, *Philips Res Rep*, 20 (1965) 528.
26 Lotgering F K, *J Phys & Chem Solids*, 27 (1996) 139.
27 O'les A, *Phys Status-Solidi a*, 3 (1970) 569.
28 Modi Kunal B, Joshi H H & Kulkarni R G, *Indain J Pure & Appl Phys*, 34 (1996) 92.